Some integrated photonics…

Jacquiline (Jacqui, Jacq) Romero

m.romero@uq.edu.au

Plan…

Introduce Hong-Ou-Mandel interference

Developments towards photonic quantum computing

Show you some inverse-designed components for a Hong-Ou-Mandel interference experiment.

VOLUME 59, NUMBER 18 PHYSICAL REVIEW LETTERS 2 NOVEMBER 1987

Measurement of Subpicosecond Time Intervals between Two Photons by Interference

C. K. Hong, Z. Y. Ou, and L. Mandel
Department of Physics and Astronomy, University of Rochester, Rochester, New York 14627
(Received 10 July 1987)

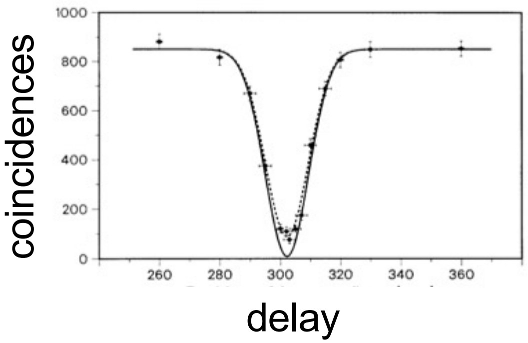

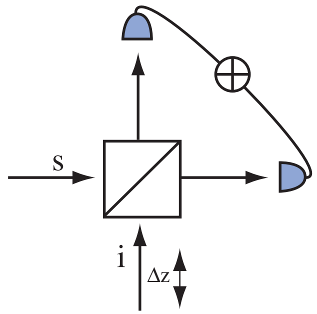

Coincidence measurement - Is there a click on BOTH photon detectors?

PHILOSOPHICAL TRANSACTIONS
OF THE ROYAL SOCIETY A

MATHEMATICAL, PHYSICAL AND ENGINEERING SCIENCES

Open Access

Check for updates

View PDF

Tools Share

Cite this article

Opinion piece

The not quite Loudon–Fearn–Rarity–Tapster dip and its impact on the development of photonic quantum information

John G. Rarity

Published: **24 December 2024** | https://doi.org/10.1098/rsta.2024.0393

2. Some mathematical details

The discovery of the destructive interference at a beamsplitter showed the utility of the creation and annihilation operator [23] formalism for describing the interactions and interference of quantum states in classical apparatus. For the purposes of this paper, we introduce the creation operators $\boldsymbol{a}_i^+$ for mode i which, when operating on a vacuum state, populates mode i with a single photon

$$\boldsymbol{a}_i^+|0\rangle = |1\rangle_i \tag{2.1}$$

Repeated operations with suitable normalization increase the photon number as in

$$\frac{\boldsymbol{a}_i^{+N}}{\sqrt{N!}}|\,0\rangle = |\,N\rangle_i\,. \tag{2.2}$$

In the opposite direction, annihilation operators $\boldsymbol{a}_i$ reduce the photon number by one. The creation and annihilation operators have commutation relation

$$\left[\boldsymbol{a}_i, \boldsymbol{a}_j^+\right] = \delta(i, j)\,. \tag{2.3}$$

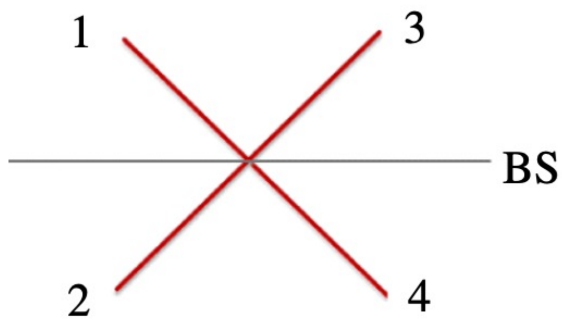

$$|\Psi_{in}\rangle = |1\rangle_1 |1\rangle_2 = \boldsymbol{a}_1^+ \boldsymbol{a}_2^+ |0\rangle .$$

$$\boldsymbol{a}_1^+ \rightarrow t\boldsymbol{a}_4^+ + i r \boldsymbol{a}_3^+ : \boldsymbol{a}_2^+ \rightarrow t\boldsymbol{a}_3^+ + i r \boldsymbol{a}_4^+ .$$

$$|\Psi_{out}\rangle = (t\boldsymbol{a}_4^+ + i r\boldsymbol{a}_3^+)(t\boldsymbol{a}_3^+ + i r\boldsymbol{a}_4^+)|0\rangle = \boxed{(t^2 - r^2)|1\rangle_3 |1\rangle_4} + \sqrt{2} irt |2\rangle_3 + \sqrt{2} irt |2\rangle_4 .$$

0 if t=r

THE UNIVERSITY OF QUEENSLAND
AUSTRALIA

Plan…

Introduce Hong-Ou-Mandel interference

Developments towards photonic quantum computing

Show you some inverse-designed components for a Hong-Ou-Mandel interference experiment.

VOLUME 73, NUMBER 1 PHYSICAL REVIEW LETTERS 4 JULY 1994

Experimental Realization of Any Discrete Unitary Operator

Michael Reck and Anton Zeilinger
Institut für Experimentalphysik, Universität Innsbruck, Technikerstrasse 25, A-6020 Innsbruck, Austria

Herbert J. Bernstein and Philip Bertani
Hampshire College and ISIS, Amherst, Massachusetts 01002
(Received 11 February 1994)

An algorithmic proof that any discrete finite-dimensional unitary operator can be constructed in the laboratory using optical devices is given. Our recursive algorithm factorizes any $N \times N$ unitary matrix into a sequence of two-dimensional beam splitter transformations. The experiment is built from the corresponding devices. This also permits the measurement of the observable corresponding to any discrete Hermitian matrix. Thus optical experiments with any type of radiation (photons, atoms, etc.) exploring higher-dimensional discrete quantum systems become feasible.

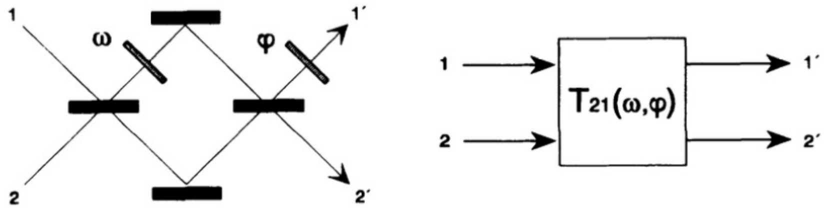

FIG. 1. A Mach-Zehnder interferometer can be used instead of a variable reflectivity beam splitter as the basic building block of any $N \times N$ unitary matrix. On the left is one experimental realization of the device using two 50:50 beam splitters, two mirrors, and two phase shifters. The Mach-Zehnder interferometer can be represented by the abstract four-port device on the right. Two parameters (ϕ, ω) of the transformation T are set in the device.

nature

Article | Published: 04 January 2001

A scheme for efficient quantum computation with linear optics

E. Knill, R. Laflamme & G. J. Milburn

Nature **409**, 46–52 (2001) | Cite this article

Going on chip…

Improves scalability and efficiency.

Improves stability (less aligning, and aligning again).

Brings quantum photonics closer to applications.

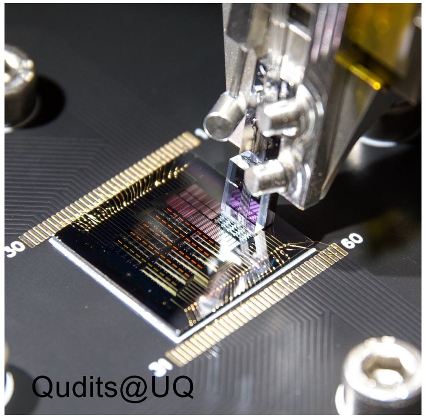

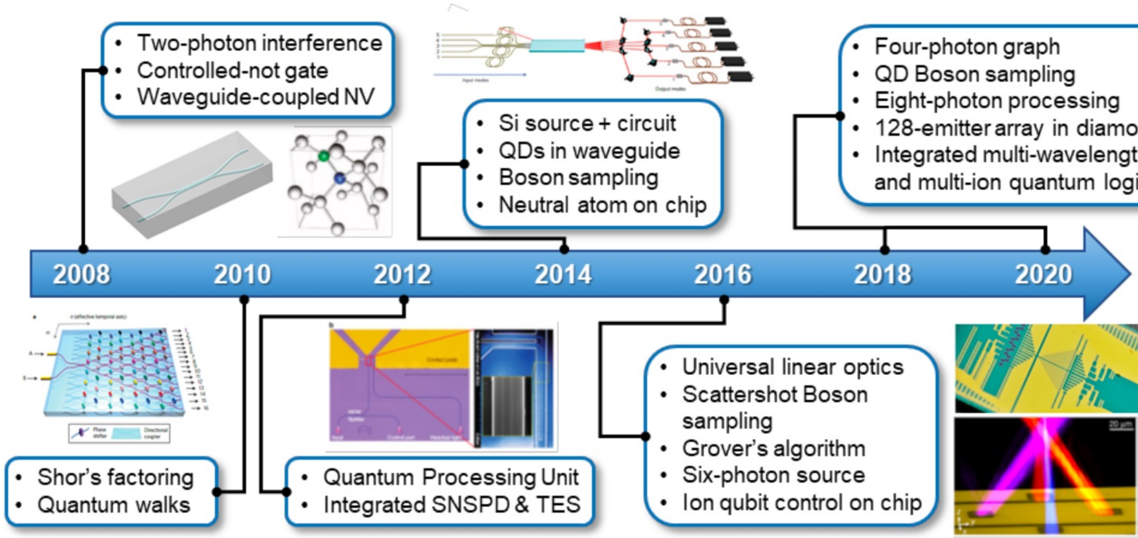

Moody et al., J Phys Photonics 4, 012501 (2022)

nature communications

THE UNIVERSITY OF QUEENSLAND
AUSTRALIA

Article

https://doi.org/10.1038/s41467-023-36493-1

Fusion-based quantum computation

Received: 19 September 2022

Accepted: 3 February 2023

Published online: 17 February 2023

Check for updates

Sara Bartolucci[1], Patrick Birchall[1], Hector Bombín[1,2], Hugo Cable[1], Chris Dawson[1], Mercedes Gimeno-Segovia[1], Eric Johnston[1], Konrad Kieling[1], Naomi Nickerson[1,2], Mihir Pant[1,2], Fernando Pastawski[1], Terry Rudolph[1] & Chris Sparrow[1]

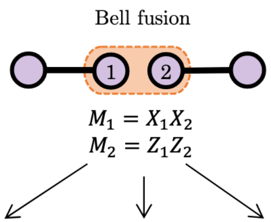

	Success	Failure	Erasure
Stabilizers measured	X_1X_2 Z_1Z_2	Z_1Z_2	None

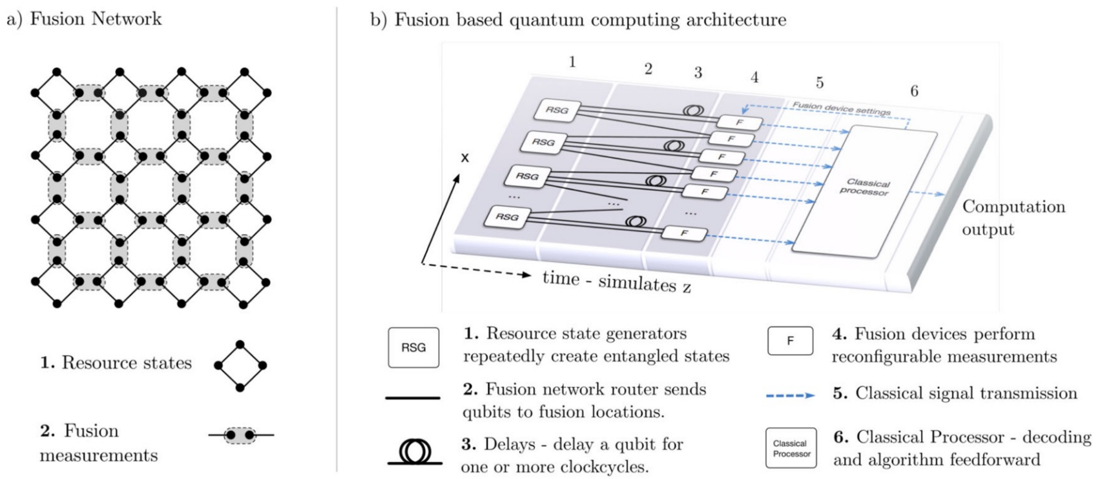

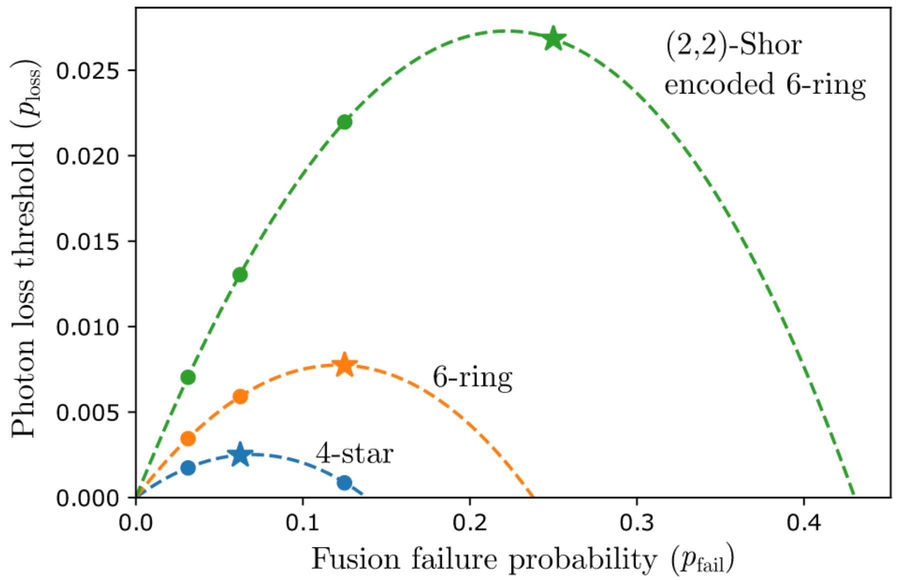

Loss has to be very low…

nature

Article | Open access | Published: 26 February 2025

A manufacturable platform for photonic quantum computing

PsiQuantum team

Nature **641**, 876–883 (2025) | Cite this article

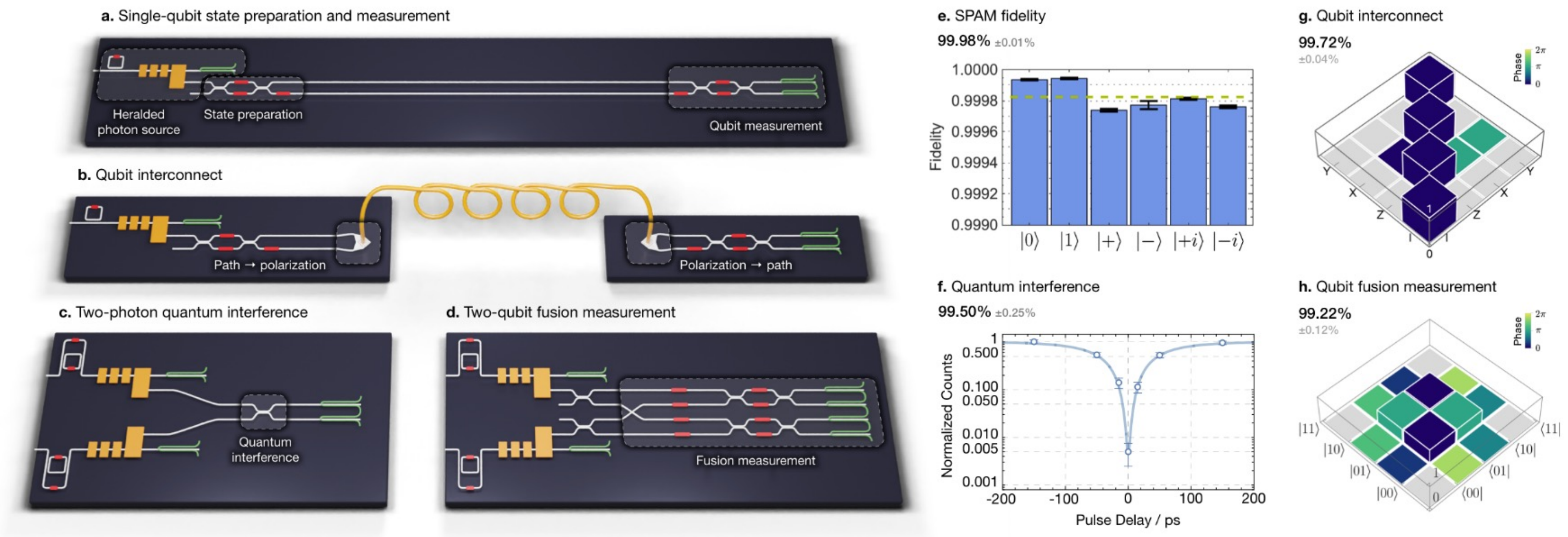

a. Single-qubit state preparation and measurement
Heralded photon source
State preparation
Qubit measurement
b. Qubit interconnect
Path → polarization
Polarization → path
c. Two-photon quantum interference
Quantum interference
d. Two-qubit fusion measurement
Fusion measurement
e. SPAM fidelity
99.98% ±0.01%
Fidelity
1.0000
0.9998
0.9996
0.9994
0.9992
0.9990
|0⟩ |1⟩ |+⟩ |−⟩ |+i⟩ |−i⟩
f. Quantum interference
99.50% ±0.25%
Normalized Counts
Pulse Delay / ps
g. Qubit interconnect
99.72%
±0.04%
Phase
h. Qubit fusion measurement
99.22%
±0.12%
Phase

a. Cascaded resonator source

b. Source JSI

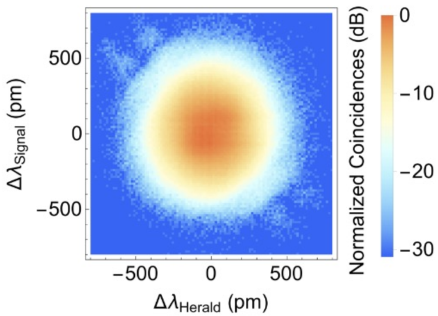

d. Photon number resolving detector

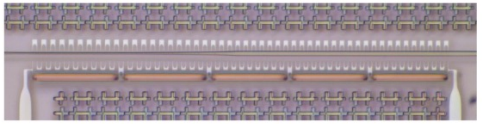

e. PNRD on-chip efficiency

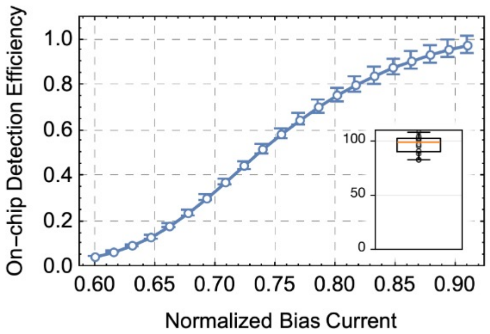

e. BTO phaseshifter cross-section

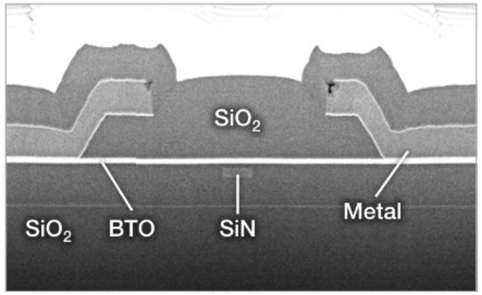

g. BTO MZI voltage response

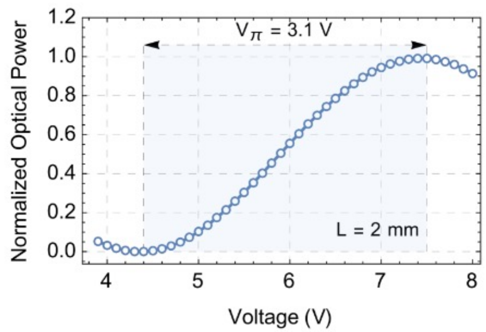


QUANDELA
QUANDELA
PRODUCTS AND SERVICES
RESOURCES
TECHNOLOGY
Driven by quantum,
empowered by Quandela
OUR APPROACH

Senellart

arXiv > quant-ph > arXiv:2412.08611

Search...

Help | Adv

Quantum Physics

[Submitted on 11 Dec 2024]

Minimizing resource overhead in fusion-based quantum computation using hybrid spin-photon devices

Stephen C. Wein, Timothée Goubault de Brugière, Luka Music, Pascale Senellart, Boris Bourdoncle, Shane Mansfield

We present three schemes for constructing a (2,2)-Shor-encoded 6-ring photonic resource state for fusion-based quantum computing, each relying on a different type of photon source. We benchmark these architectures by analyzing their ability to achieve the best-known loss tolerance threshold for fusion-based quantum computation using the target resource state. More precisely, we estimate their minimum hardware requirements for fault-tolerant quantum computation in terms of the number of photon sources to achieve on-demand generation of resource states with a desired generation period. Notably, we find that a group of 12 deterministic single-photon sources containing a single matter qubit degree of freedom can produce the target resource state near-deterministically by exploiting entangling gates that are repeated until success. The approach is fully modular, eliminates the need for lossy large-scale multiplexing, and reduces the overhead for resource-state generation by several orders of magnitude compared to architectures using heralded single-photon sources and probabilistic linear-optical entangling gates. Our work shows that the use of deterministic single-photon sources embedding a qubit substantially shortens the path toward fault-tolerant photonic quantum computation.

Plan…

Introduce Hong-Ou-Mandel interference

Developments towards photonic quantum computing

Show you some inverse-designed components for a Hong-Ou-Mandel interference experiment.

Transverse modes as qudits

	Generation	Processing	Measurement and detection
Free-space	Spatial light modulator (SLM) spontaneous parametric down-conversion (SPDC)	Multi-plane light conversion (MPLC)	Spatial light modulator and single photon detection (mode filtering + single-photon detection)
On-chip			

Multiplexer for transverse modes on-chip

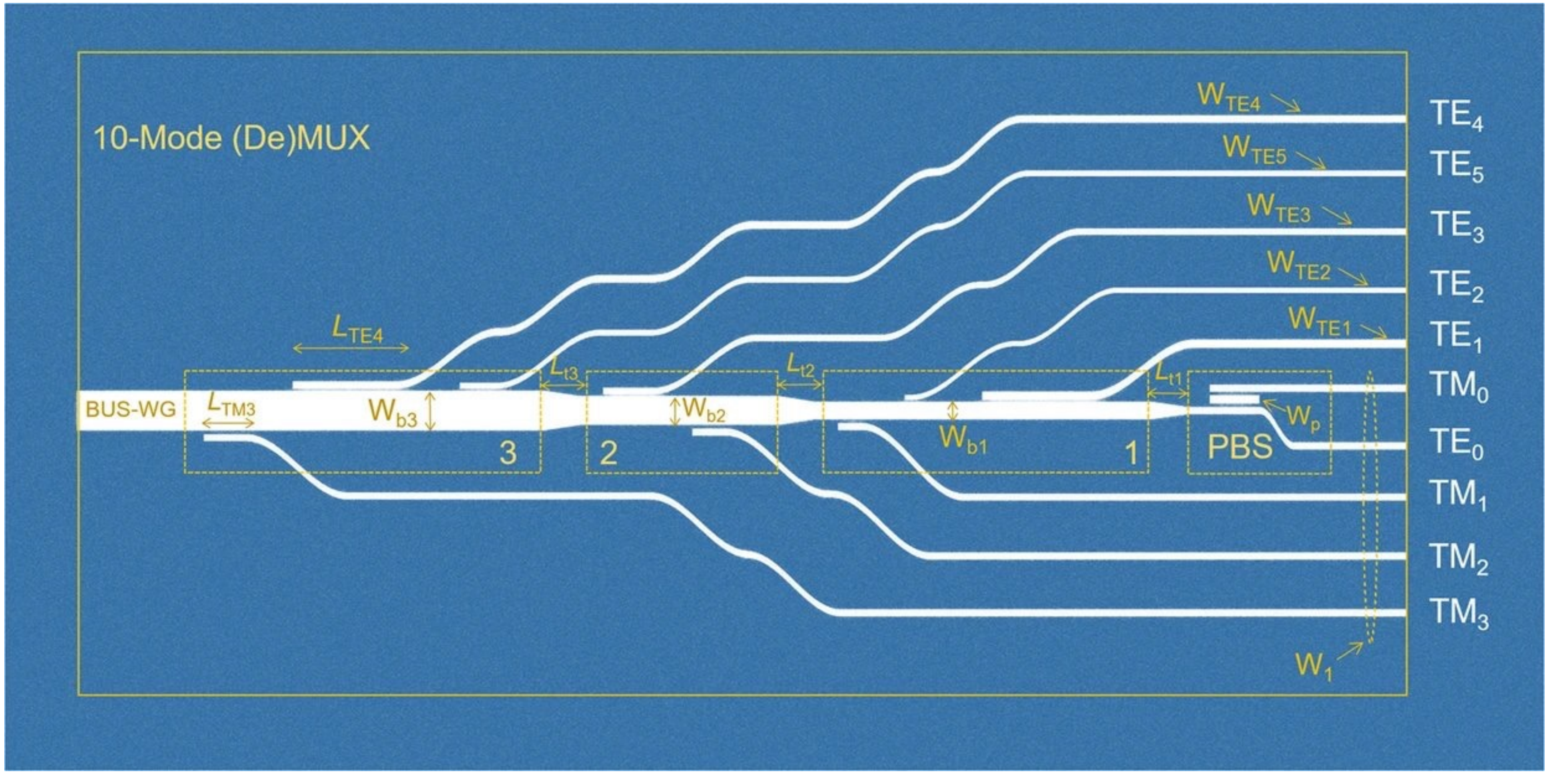

Jiang, et al. *Scientific Reports 2019 9:1*, *9*(1), (2019).

Photonic inverse design

Design by specification (just like MPLC)

User defines input and desired function and algorithm finds optimal design

Can increase device performance and robustness and decrease footprint

In comparison to traditional methods of tuning a handful of device parameters, inverse design utilizes entire parameter space

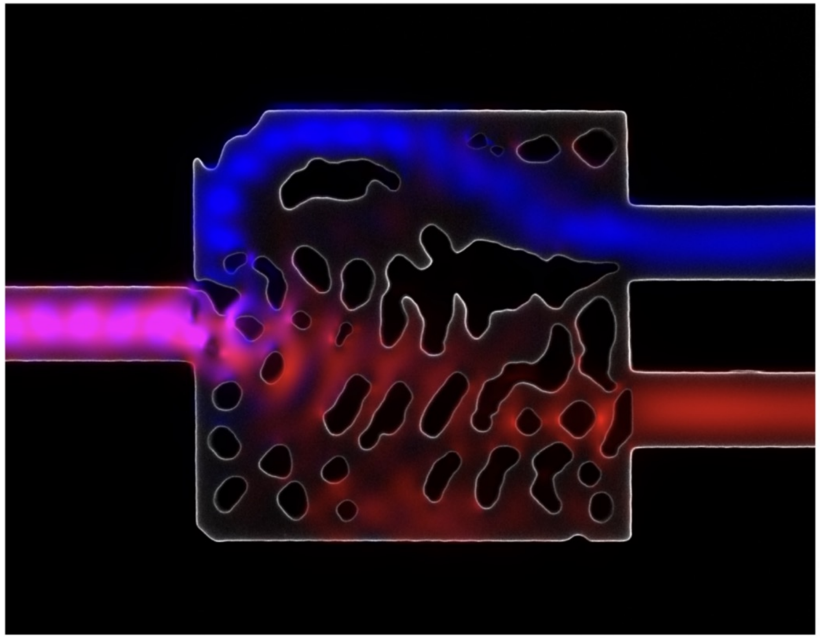

L., *et al. Applied Physics Reviews*, 7(1), 011407 (2020)

Photonic inverse design

Jamika Roque

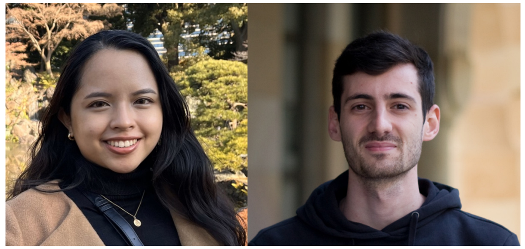

Daniel Peace

Optimisation of device topology with respect to some figure of merit by repeatedly performing 2D / 3D electromagnetic simulations. Uses gradient descent-based optimisation using the adjoint method.

Fabrication constraints can be set. Robust to fabrication error.

Objective function

$$\min_{p} f_{obj}(\boldsymbol{p}) = \left(\left|c^{\dagger}\boldsymbol{E}(\boldsymbol{p})\right| - t\right)^{2}$$

Overlap between electric field $\boldsymbol{E}$ and target mode c

Target transmission

$\boldsymbol{p}$ – parameterisation vector which controls the permittivity distribution $\epsilon(\boldsymbol{p})$ of the design area

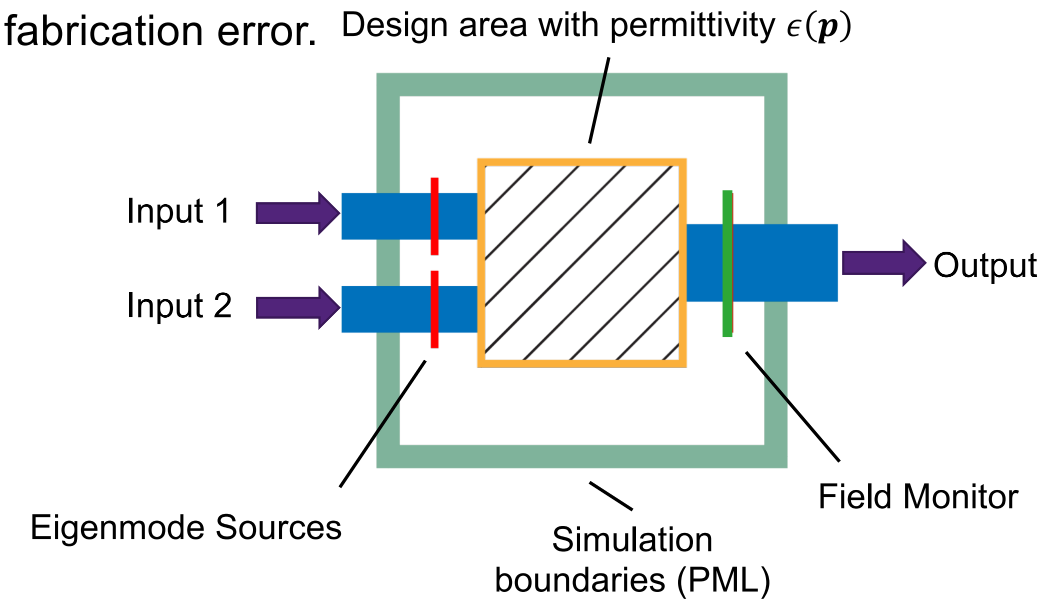

Su, L., *et al. Applied Physics Reviews*, 7(1), 011407 (2020)

Mode (De)Multiplexer

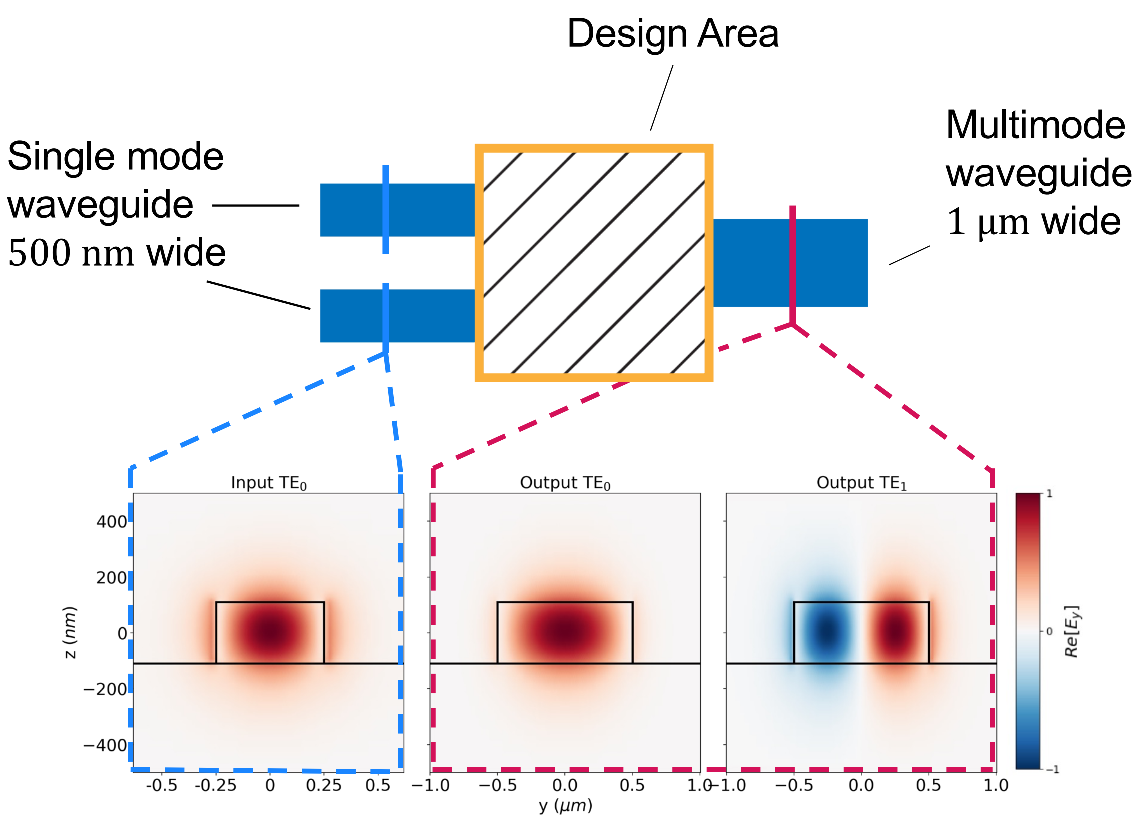

Peace et al., FiO 2024

Mode (De)Multiplexer

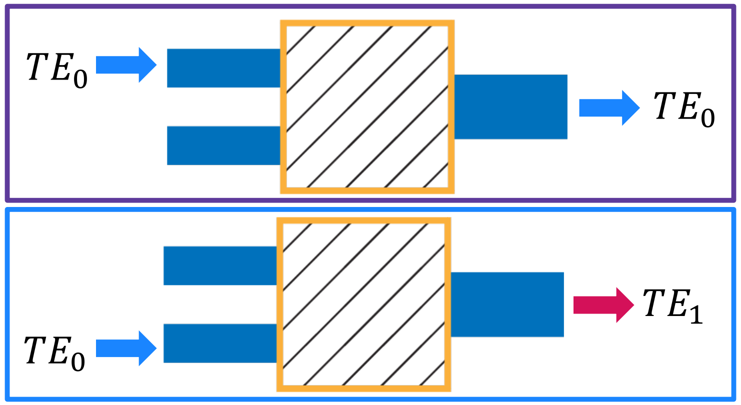

Objective function

$$f_{obj}(\boldsymbol{p}) = \left(\left|c^{\dagger}_{a,n}\boldsymbol{E_n}(\boldsymbol{p})\right| - t\right)^2$$

where, $a = 0{,}1$ (input waveguide)
$n = 0{,}1$ (output mode)

$$f_{obj}(\boldsymbol{p}) = \left(\left|c^{\dagger}_{0,0}\boldsymbol{E_0}(\boldsymbol{p})\right| - 1\right)^2 + \left(\left|c^{\dagger}_{0,1}\boldsymbol{E_1}(\boldsymbol{p})\right| - 0\right)^2 + \left(\left|c^{\dagger}_{1,1}\boldsymbol{E_1}(\boldsymbol{p})\right| - 1\right)^2 + \left(\left|c^{\dagger}_{1,0}\boldsymbol{E_0}(\boldsymbol{p})\right| - 0\right)^2$$

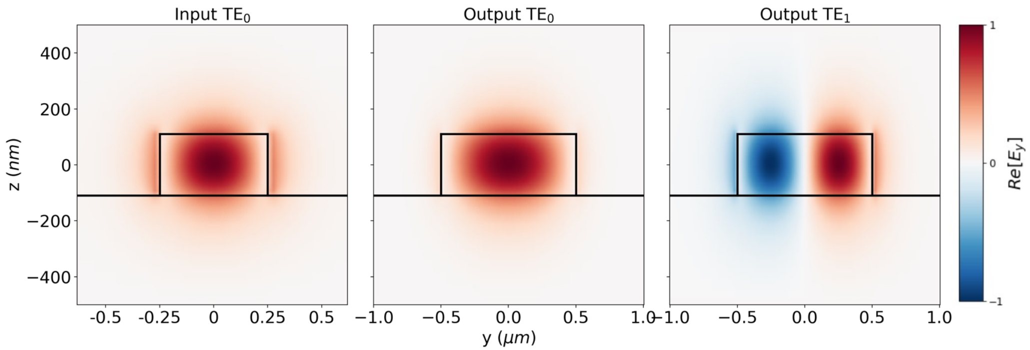

Peace et al., FiO 2024

Mode (De)Multiplexer

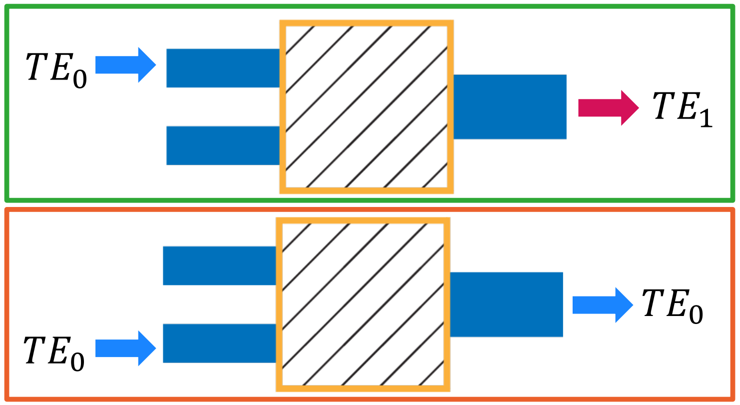

Objective function

$$f_{obj}(\boldsymbol{p}) = \left(\left|c_{a,n}^{\dagger}\boldsymbol{E_n}(\boldsymbol{p})\right| - t\right)^2$$

where, $a = 0,1$ (input waveguide)
$n = 0,1$ (output mode)

$$f_{obj}(\boldsymbol{p}) = \left(\left|c_{0,0}^{\dagger}\boldsymbol{E_0}(\boldsymbol{p})\right| - 1\right)^2 + \left(\left|c_{0,1}^{\dagger}\boldsymbol{E_1}(\boldsymbol{p})\right| - 0\right)^2 + \left(\left|c_{1,1}^{\dagger}\boldsymbol{E_1}(\boldsymbol{p})\right| - 1\right)^2 + \left(\left|c_{1,0}^{\dagger}\boldsymbol{E_0}(\boldsymbol{p})\right| - 0\right)^2$$

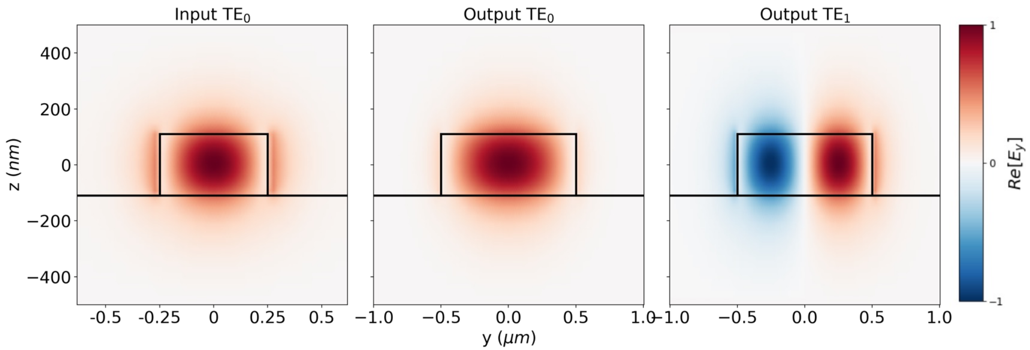

Peace et al., FiO 2024

Mode (De)Multiplexer

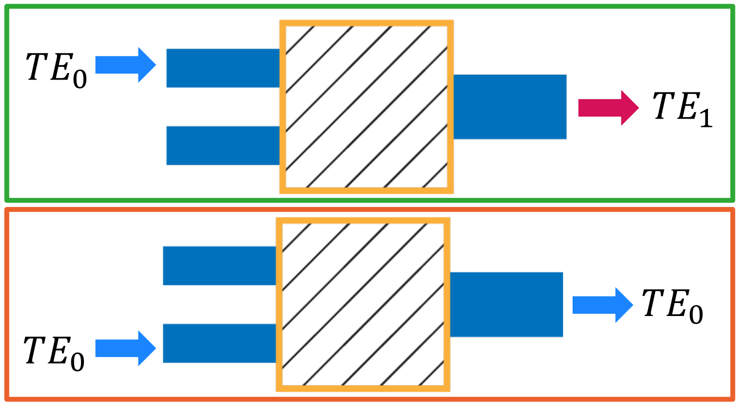

Objective function

$$f_{obj}(\boldsymbol{p}) = \left(\left|c^{\dagger}_{a,n}\boldsymbol{E_n}(\boldsymbol{p})\right| - t\right)^2$$

where, $a = 0{,}1$ (input waveguide)
$n = 0{,}1$ (output mode)

$$f_{obj}(\boldsymbol{p}) = \left(\left|c^{\dagger}_{0,0}\boldsymbol{E_0}(\boldsymbol{p})\right| - 1\right)^2 + \left(\left|c^{\dagger}_{0,1}\boldsymbol{E_1}(\boldsymbol{p})\right| - 0\right)^2 + \left(\left|c^{\dagger}_{1,1}\boldsymbol{E_1}(\boldsymbol{p})\right| - 1\right)^2 + \left(\left|c^{\dagger}_{1,0}\boldsymbol{E_0}(\boldsymbol{p})\right| - 0\right)^2$$

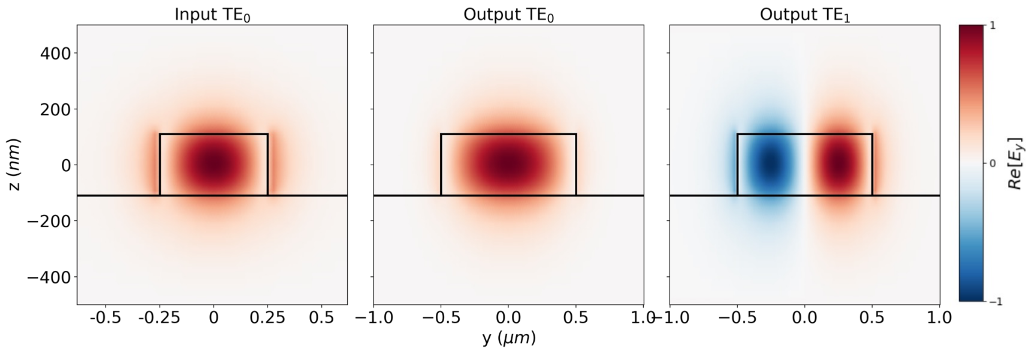

Design area = 3 μm×3 μm
Simulation area = 7 μm×7 μm

Runtime: ~8 hours for 100 iterations
with a 40 nm mesh resolution

Peace et al., FiO 2024

Mode (De)Multiplexer

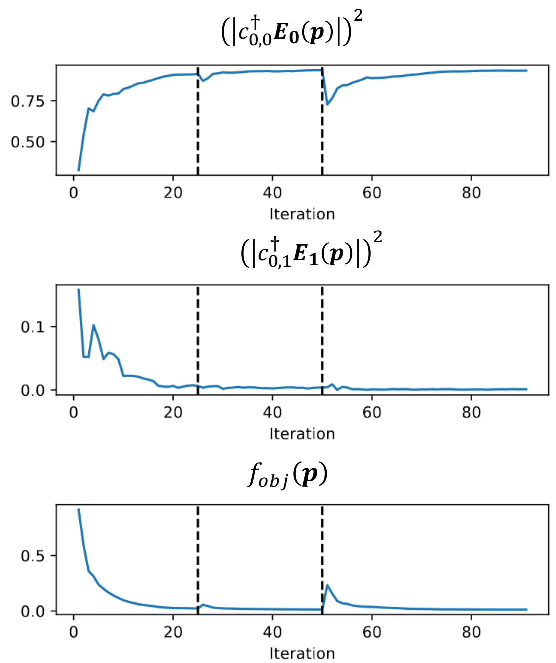

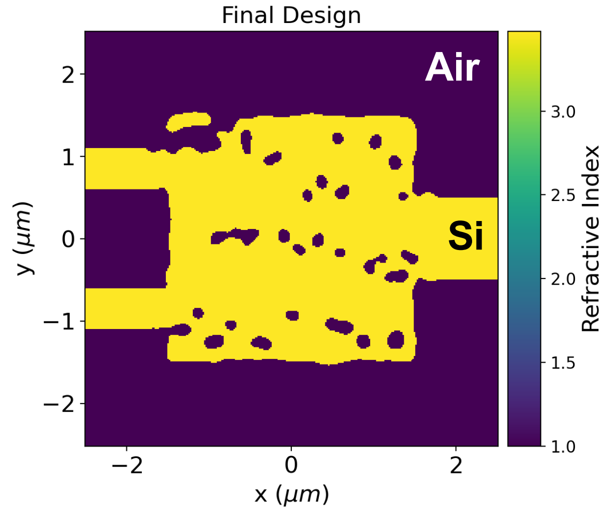

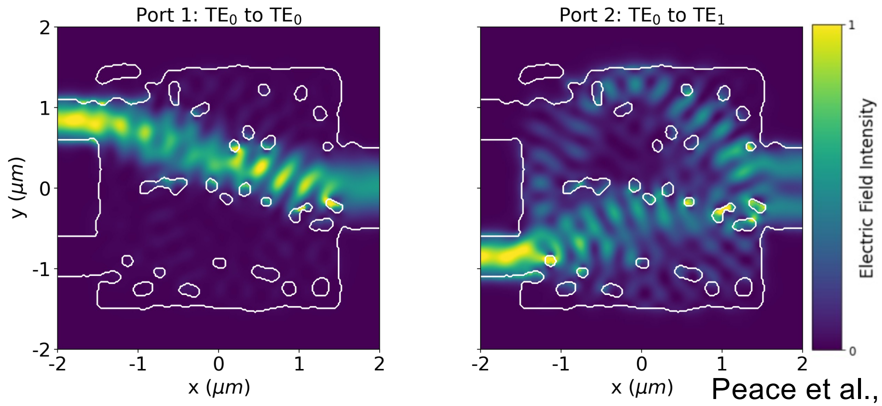

Peace et al., FiO 2024

Simulated

Port 1: TE_0 to TE_0	93.4% Transmission, -29.1 dB Crosstalk
Port 2: TE_0 to TE_1	91.2% Transmission, -30.1 dB Crosstalk

Mode (De)Multiplexers

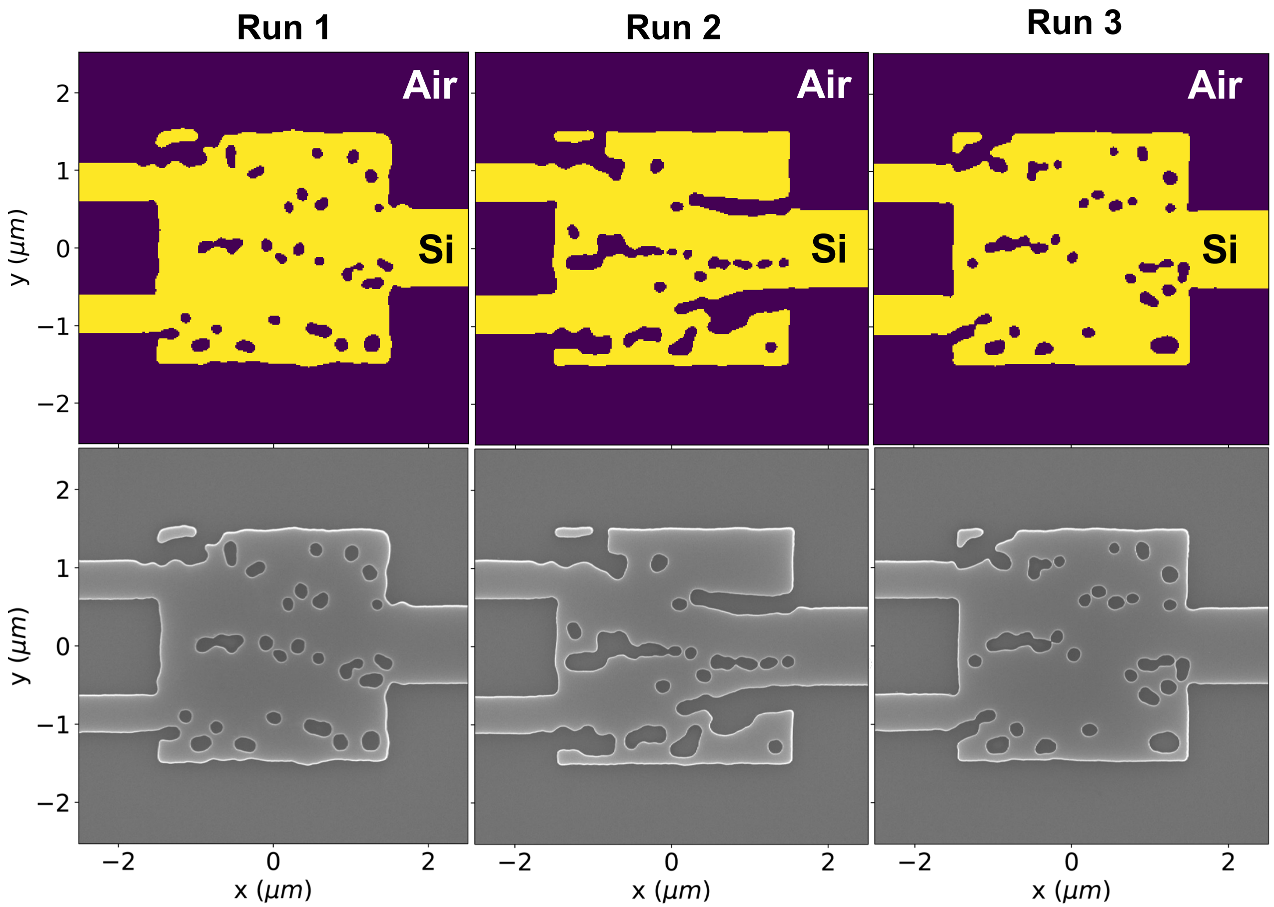

Simulated

Run 1	Transmission	Crosstalk
Port 1	93.4%	-29.1 dB
Port 2	91.2%	-30.1 dB

Run 2	Transmission	Crosstalk
Port 1	96.5%	-33.7 dB
Port 2	92.4%	-30.2 dB

Run 3	Transmission	Crosstalk
Port 1	92.8%	-28.8 dB
Port 2	88.9%	-30.1 dB

Peace et al., FiO 2024

Mode Beamsplitters

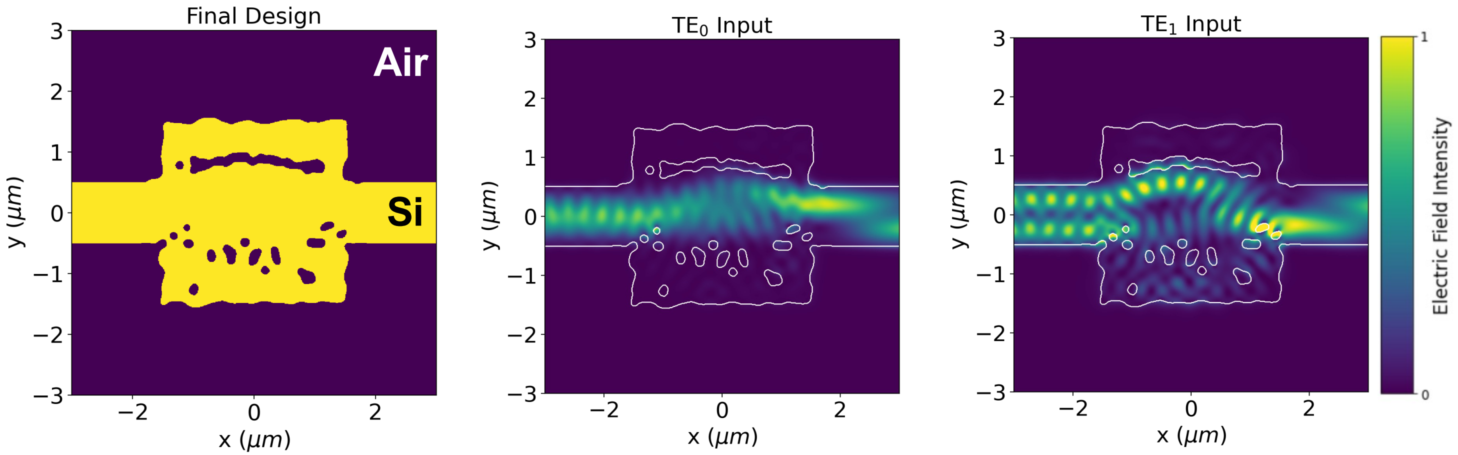

Simulated

TE_0 Input

TE_0 47.8% TE_1 48.2%

TE_1 Input

TE_0 46.1% TE_1 46.8%

Peace et al., FiO 2024

Hong-Ou-Mandel (HOM) Interference

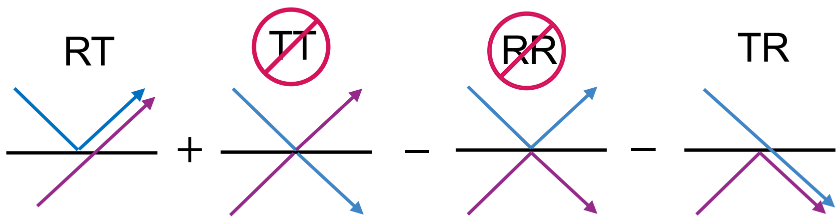

Hong, Ou, Mandel, *Phys. Rev. Lett. 59*, 2044 (1987)

Visibility= 95 ± 0.02%

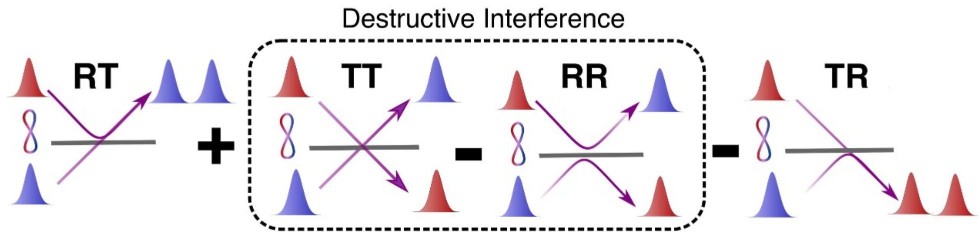

Joshi et a., *Phys. Rev. Lett. 124*, 143601 (2020)

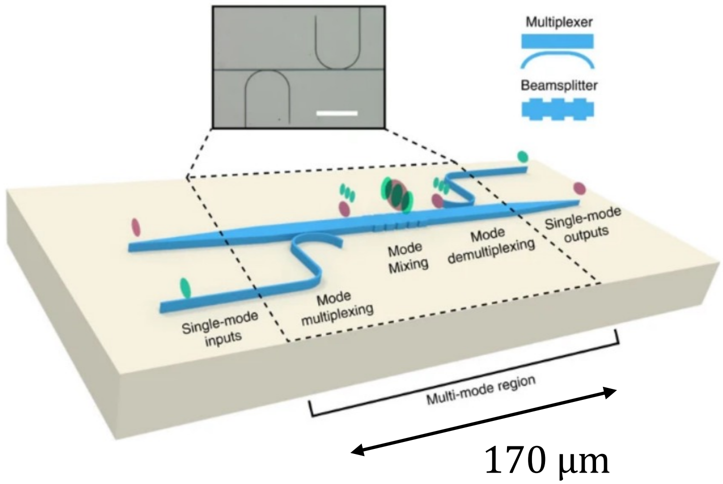

Inverse design can reduce this footprint.

Mohanty, A., *et al. Nature Communications*, *8*(1), 14010. (2017)

Hong-Ou-Mandel (HOM) Interference

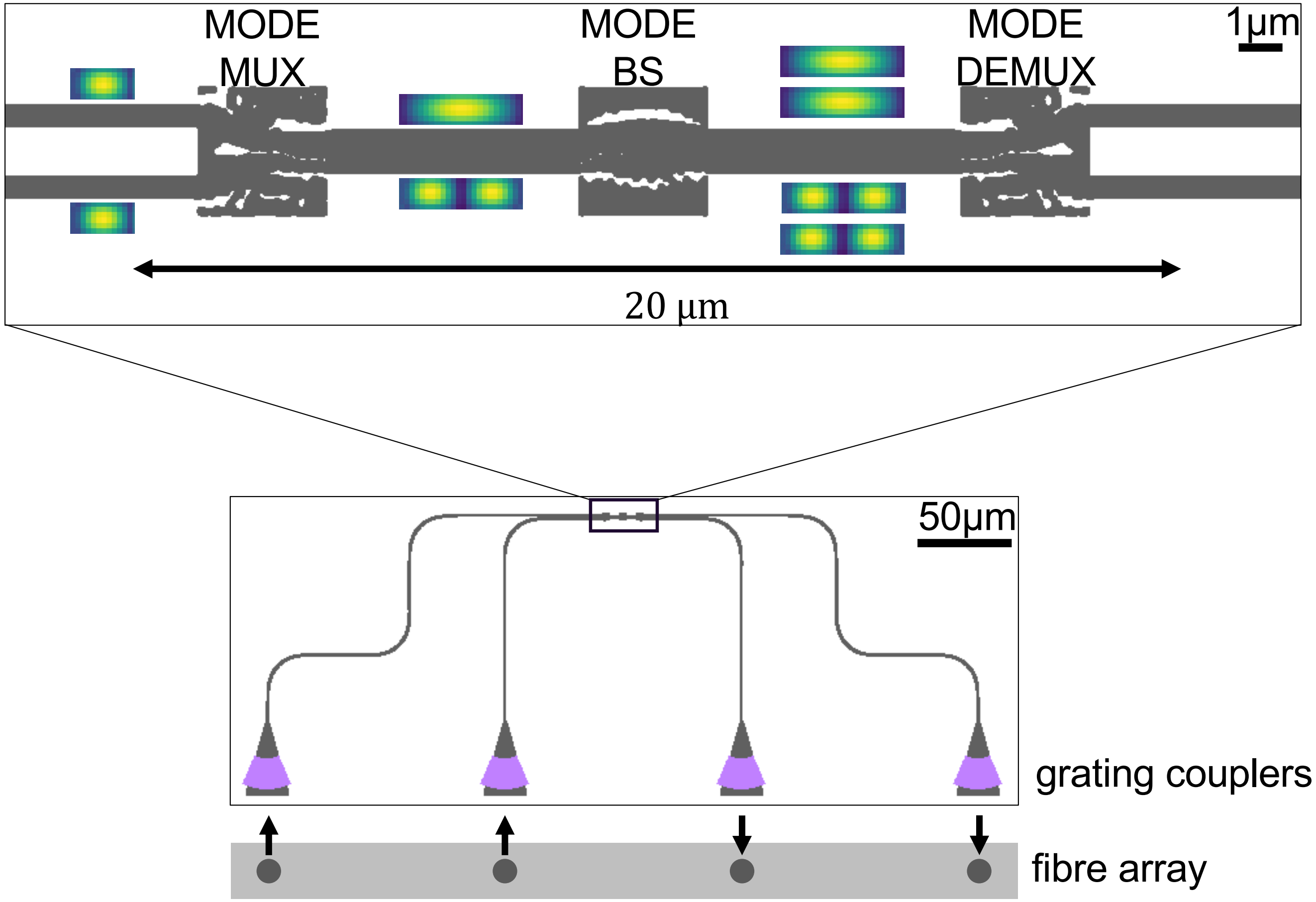

Peace et al., FiO 2024

Testing Hong-Ou-Mandel (HOM) Interference

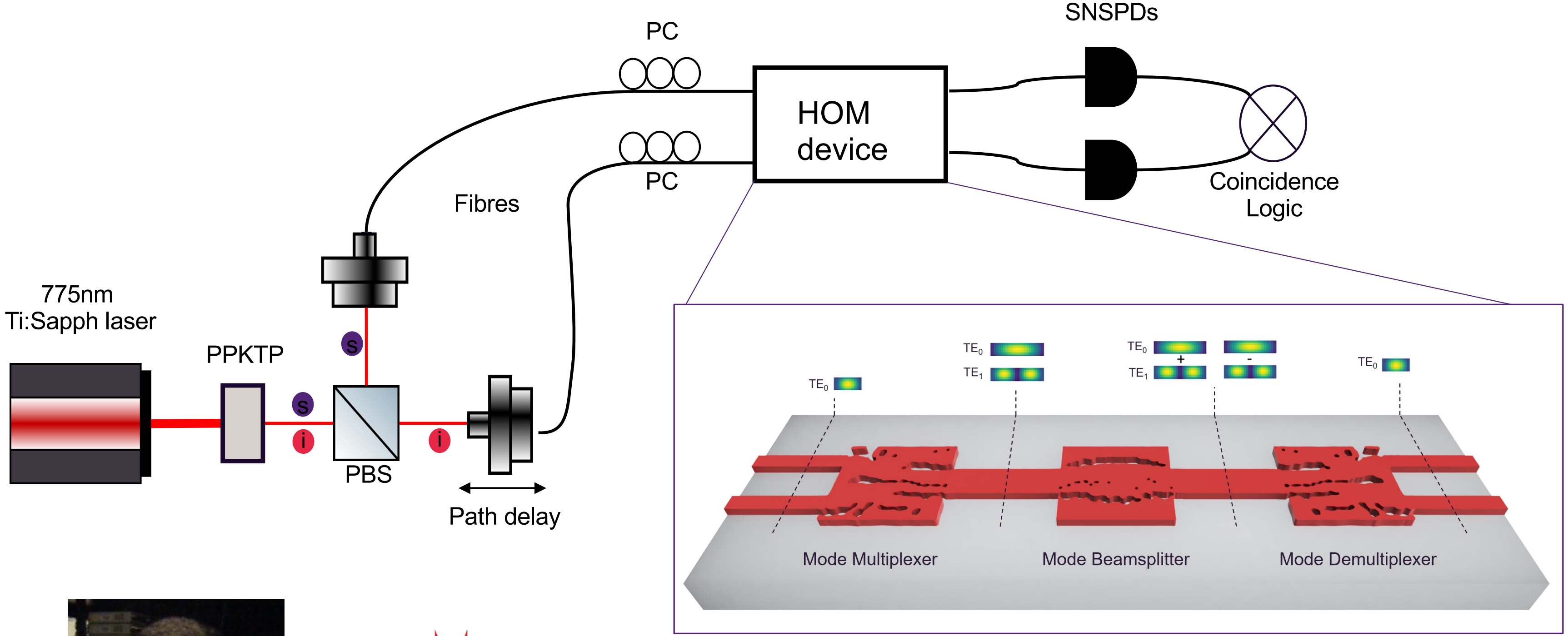

Nora Tischler

Farzad Gharafi

Griffith UNIVERSITY Queensland, Australia

Peace et al., FiO 2024

On-chip HOM interference

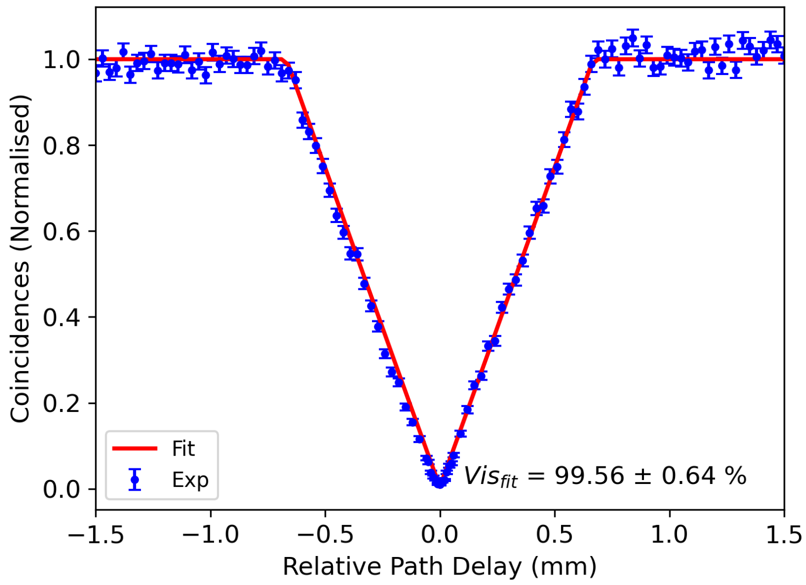

Good HOM visibility, no degradation from the measured source visibility.

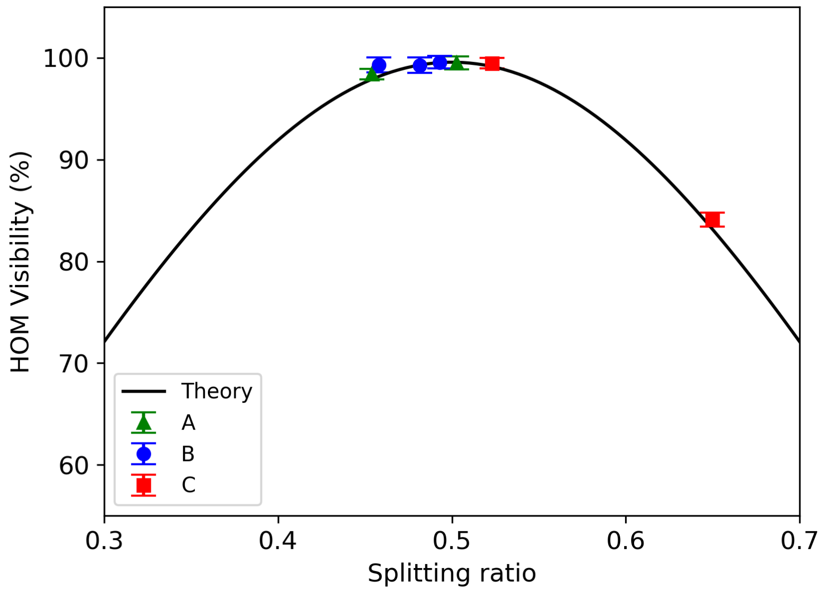

Good HOM visibility across different designs and devices.

We can model the visibility.

Peace et al., FiO 2024

Fabrication bias simulation

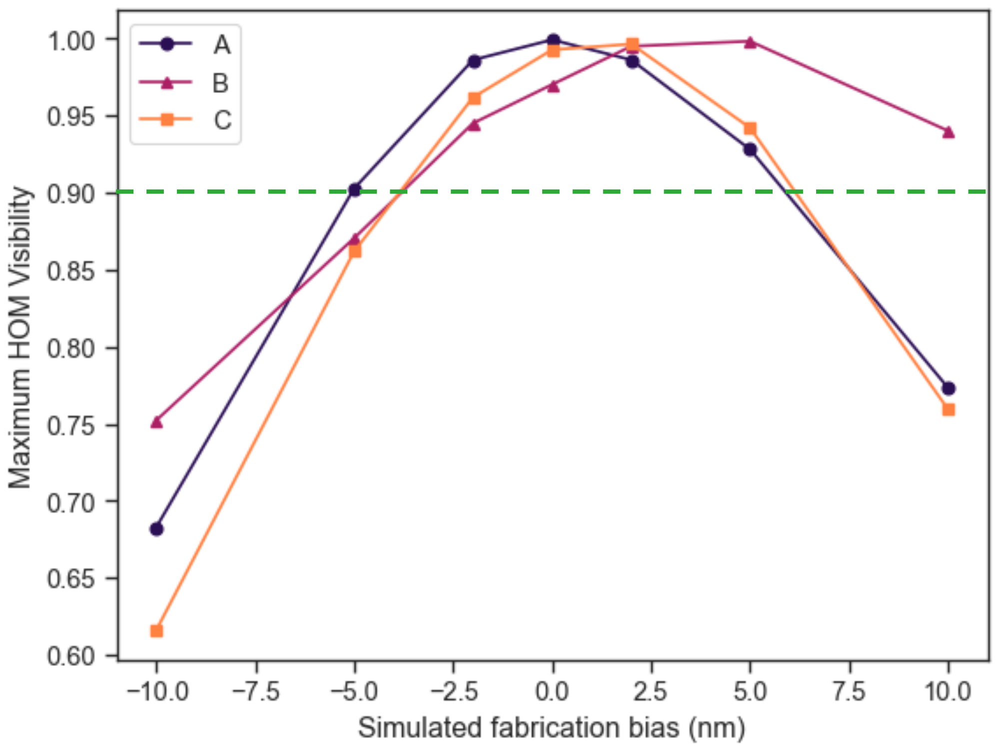

>90% visibility for 5 nm bias

>50% visibility for >10 nm bias

Take home…

- Hong-Ou-Mandel interference is a quintessential quantum optics phenomenon, very important for linear optical quantum computing.

- We have made some huge strides towards fault-tolerant quantum computing, very active field.

- Inverse design can be a reliable way to design components for quantum information processing.

Thank you!